

Preparation and characterization of ceramic sol–gel composite coatings - densification temperature optimisation -

Ouafa TAHIRI ALAOUT¹, Matthieu TOUZIN² and Franck BECLIN²

¹ *Département de chimie, Faculté des Sciences et Techniques, Université My Ismail, BP 509 Boutalamine, Errachidia, Morocco*

² *Unité Matériaux et Transformations, Université de Lille 1- Bâtiment C6, 59655 Villeneuve d'Ascq*

Abstract: Thick (~ 25 µm) ceramic coatings on porous ceramic substrates were elaborated by means of dispersing alumina and rutile powders in a silica sol-gel solution. Resulting coatings, which present a composite structure consisting in Al₂O₃ and TiO₂ grains embedded in an amorphous SiO₂ matrix, demonstrate a good adhesion to the substrate and a real improvement of its surface by closing the porosity and also reducing the roughness. Mechanical characterization by micro-indentation showed an increase of the coating hardness when the thermal treatment temperature increases. This hardness increase is attributed to the densification of the coating that proceeds by grain rearrangement thanks to the sol-gel derived silica phase viscosity decrease during the thermal treatment. In order to decrease the coating densification temperature, the silica intergranular phase was modified by incorporating Na⁺ ions in its structure. This was done by adding NaCl salt in the sol-gel solution and leads to the decrease of the densification temperature.

Keywords: sol-gel processing, coating, thermal treatment, hardness, sodium chloride.

I. Introduction

The importance of porous materials has been recognized since antiquity when porous charcoal was used for its medicinal properties [1]. The worldwide interest [2] in environmental protection and energy conservation has revived the research on porous materials, which have numerous applications such as in catalysis, separation, insulation, sensors, and chromatography. Moreover, porous ceramic materials present many other interests such as lightness, thermal shock resistance or thermal insulation...[1]. Nevertheless, surface open porosity and the induced high roughness can be unfavourable for some applications. In these cases, it is then necessary to modify these materials to obtain a smooth surface devoid of porosity and roughness. Among the different available coating processes, the sol-gel technology provides some advantages. Indeed, the sol-gel has long been known [3-4] and it offers many strengths to produce materials of high homogeneity and purity, at lower temperatures than conventional methods [5]. This process does not involve the melting or sintering of ceramic powders to produce, but uses a precursor solution containing reagents such as alkoxides or metal salts. Moreover, producing coatings by this method presents a lot of advantages such as low temperature, cost effectiveness and the possibility of coating different substrate materials and complex geometries. Despite its advantages, sol-gel technology has never reached its full industrial potential for many applications, due to thickness and substrate limitations. Individual coating layers are limited to less than 0.5 µm to prevent cracking and coating failure resulting from trapped organics within the coating during thermal processing. The sol-gel method is also highly substrate-dependent,

primarily due to limitations imposed by thermal mismatch between the coating and the substrate. The combination of these two factors usually prevents the overall coating thickness from being greater than 10 µm.

In this study, in order to correct the roughness and block the surface porosity of highly porous materials, the sol gel processing has been modified by the addition of ceramic powders in the sol-gel solution to increase the coating thickness while preventing the cracking [2-3-6]. This “novel” method of coating (sol-gel composite) developed by Barrow and Petroff [7] consists in dispersing ceramic powders in a sol-gel solution. This suspension can then be spray, dip or spin-deposited on a substrate. Upon firing, the sol-gel derived phase acts to bind the powder phase internally and the overall coating to the substrate. Crack-free adherent film layers up to 25 µm thick can be deposited, with the option of multiple depositions leading to an overall coating thickness in excess of 500 µm.

In this article, we describe the preparation and the resulting microstructure of Al₂O₃/TiO₂/SiO₂ composite coatings prepared by the “sol-gel composite” method and deposited on highly porous ceramic substrates in order to improve their surface state. Moreover, to diminish the elaboration temperature of the coatings, the composition of the sol-gel derived intergranular phase is modified by the addition of NaCl salt. The effect of this modification on the densification temperature is characterized by means of microhardness measurements.

II. Experimental section

2.1. Chemicals and elaboration protocol

Tetraethoxysilane (TEOS, 98 %, Acros Organics, Belgium), alumina (ALMATIS, average grain size from 1

to 1.4 μm), titanium dioxide (rutile form, ART E COLOR, average grain size of $0.5 \pm 0.02 \mu\text{m}$), hydrochloric acid (HCl, 1N, Acros Organics, Belgium), ethanol (Prolabo, 99,5%) and sodium chloride salt (NaCl, Carlo Erba Reactifs Sds, 99%) were used as raw materials.

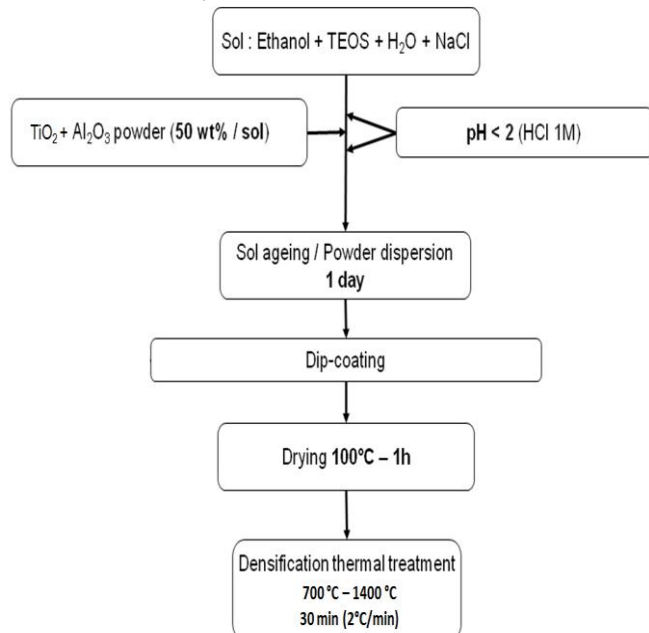


Fig. 1: $\text{TiO}_2/\text{SiO}_2/\text{Al}_2\text{O}_3$ coating preparation protocol

$\text{TiO}_2/\text{Al}_2\text{O}_3/\text{SiO}_2$ coatings were prepared by following the steps described in the flowchart shown in Fig.1. Firstly, the sol-gel solution is prepared: silica precursor TEOS is mixed with ethanol, water is then added to the mixture in order to activate hydrolysis-condensation reactions, the molar ratio Water/TEOS/Ethanol was optimized in a previous study and corresponds to 4/1/6 [8]. The pH of the solution is fitted to 1.8 by the addition of some drips of HCl. Acid catalysis conditions promote weakly-branched polymeric structure that is favourable to produce a continuous phase [9]. Under magnetic stirring, NaCl salt is added in solution with various Na/Si molar ratios ranging from 0.0 to 0.43, while checking the pH. Then alumina and rutile powders are added with $\text{Al}_2\text{O}_3/\text{TiO}_2$ molar ratio of 0.7 and a powder/solution weight ratio of 1/1. The pH is maintained to 1.8 in order to promote a good dispersal of the powder. The stirring is maintained during 24 h to reach good mixture homogeneity. The substrates used in this work are aluminosilicate materials containing about 30 % of partially open porosity and presenting an important surface roughness as shown in fig.2. The pore size is about 25 μm . The substrate samples are 1 mm thick and present a surface area of about 0.5 cm^2 . Samples are first cleaned under ultrasounds in acetone (99.5 %) for 15 min and then in distilled water for 15 min. Deposition is made by dipping in the sol-gel composite solution. After immersion

during 1s, samples are withdrawn with a speed of 5mm/s. Coated samples are then dried at 100 °C for 1 hour and heat-treated at various temperatures (from 700°C, up to 1400 °C) for 30 min in air at a heating and cooling rate of 2°C/min. In order to obtain thick layers, three coatings are made by following the same procedure.

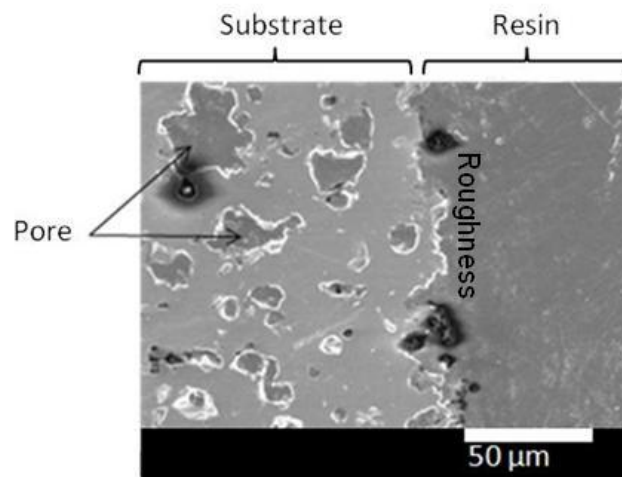


Fig.2: State of surface substrate ceramic before $\text{TiO}_2/\text{SiO}_2/\text{Al}_2\text{O}_3$ coating

2.2. Coating characterization

The surface morphology and cross-section studies were performed by scanning electron microscopy (SEM, Hitachi S4700).

The micro-hardness tester (MHT, CSM Instruments SA) was chosen as an instrumented indentation system that allows measurements of mechanical properties by controlling the charge as a function of depth at high resolution. In this study, a maximum load of 500mN is applied on the sample with a speed of 1N/min, the maximum load is maintained during 15s.

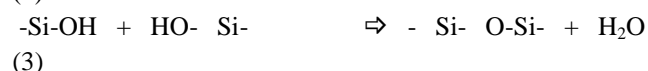
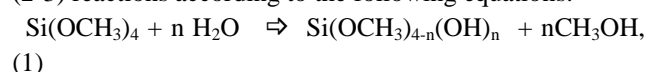
The hardness of testing samples was derived from the load–displacement curve following the Oliver and Pharr scheme [10].

About 25 hardness measurements were performed in several places on large sections polished for more reproducible results.

III. Results and discussion

3.1. Morphological characterization of coatings

Gelation is the result of hydrolysis (1) and condensation (2-3) reactions according to the following equations:



During drying at 100 °C and firing at higher temperature reactions 2 and 3 go to completion and the gel shrinks to a densified product.

In order to investigate the surface morphology of elaborated coatings before and after heat treatment, SEM was used to observe the $\text{TiO}_2/\text{Al}_2\text{O}_3/\text{SiO}_2$ composite films. Fig.3 presents the surface coating before (Fig.3a) and after (Fig.3b) thermal treatment. It shows that the surface coating is relatively smooth and homogeneous, fine rutile ($0.5 \pm 0,02 \mu\text{m}$) and coarser alumina ($1 \pm 0,5 \mu\text{m}$) grains are well dispersed in the SiO_2 gel. It is also interesting to notice that both coatings are crack-free. Comparison between these two pictures highlights the role of the sol-gel derived phase on the densification of the coating. Indeed, a significant porosity decrease after treatment at 1200°C (Fig.3b) is noted. Moreover it is obvious that the ceramic grains are well coated by the silica phase (Fig. 3b).

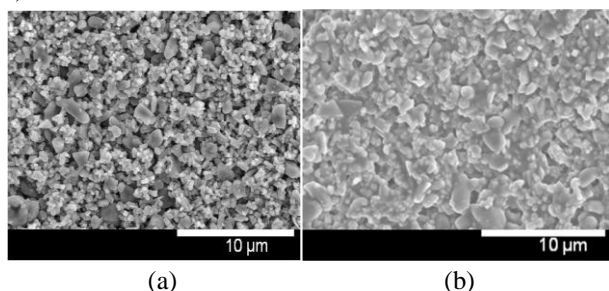


Fig. 3: SEM observation of the surface coating (a) before and (b) after densification at 1200 °C, $\text{Al}_2\text{O}_3/\text{TiO}_2 = 0.7$

Fig.4 presents the SEM cross-section picture of a $\text{TiO}_2/\text{Al}_2\text{O}_3/\text{SiO}_2$ coating. Its thickness can be estimated to ca. 25μm. It shows a uniform distribution of porosity with a mean pore size of about 0.5 μm. The coating closes the surface porosity of the substrate and also reduces its roughness. The interface between the coating and the substrate seems to present good adhesion properties. In addition, visual observation shows that the rutile addition in the mixture improves the coating aesthetic properties by increasing its brightness.

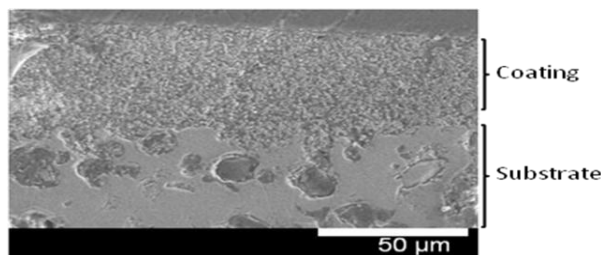


Fig.4: SEM observation of a coating cross-section after densification at 1200 °C, $\text{Al}_2\text{O}_3/\text{TiO}_2 = 0.7$

3.2. Mechanical characterization of coatings

In this section, the influence of the heat treatment on the coating mechanical properties, especially the Vickers micro-hardness, is studied. Fig. 5 shows the typical view of an indent print. The hardness evolution of the $\text{TiO}_2/\text{Al}_2\text{O}_3/\text{SiO}_2$ coating densified at different heat treatment temperatures is shown in fig. 6. It shows a small increase of the hardness, from 190Hv to 300Hv, between 700°C and 1200°C. We note, between 1200°C and 1400 °C, a strong increase of the coating hardness that goes from 300Hv to 680Hv. This evolution can be explained by the structural change of the coating during the thermal treatment. For a composite material the hardness measured result of the sum of the different hardness of each phase. In comparison with the hardness of alumina ($1519 \pm 31 \text{ Hv}$ [11]), rutile ($\sim 1100 \text{ Hv}$ [12]) and fused silica ($\sim 900 \text{ Hv}$ [13]), the relative low hardness values measured for coating annealed at below 1200°C is due to the residual porosity. Up to 1000°C, the main evolution of the microstructure is due to the drying and the densification of the gel which induce the low shrinkage of the coating shown in the figure 7a; 7b; 7c. Between 1000 to 1200°C the gel to glass transition occur [14-15]. The smooth hardness evolution of the annealing temperatures going from 700 to 1200°C is due to the shrinkage of the coating induced by the densification of the gel.

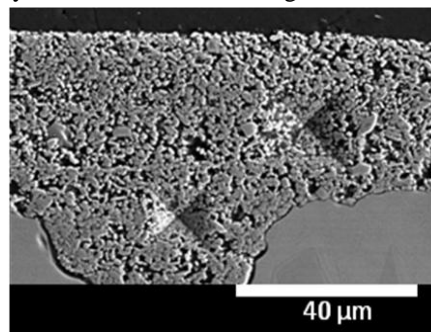


Fig.5: Typical view of an indent print

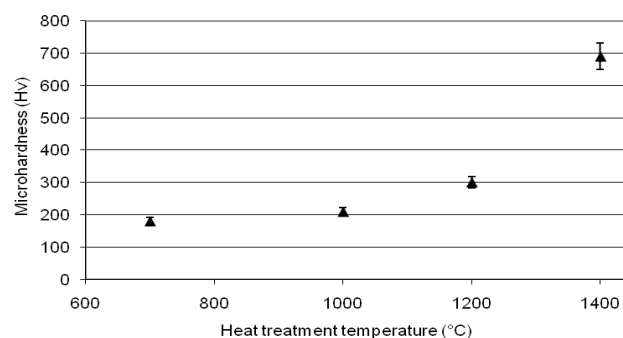


Fig.6: Effect of heat treatment temperature on the $\text{TiO}_2/\text{SiO}_2/\text{Al}_2\text{O}_3$ coating hardness.

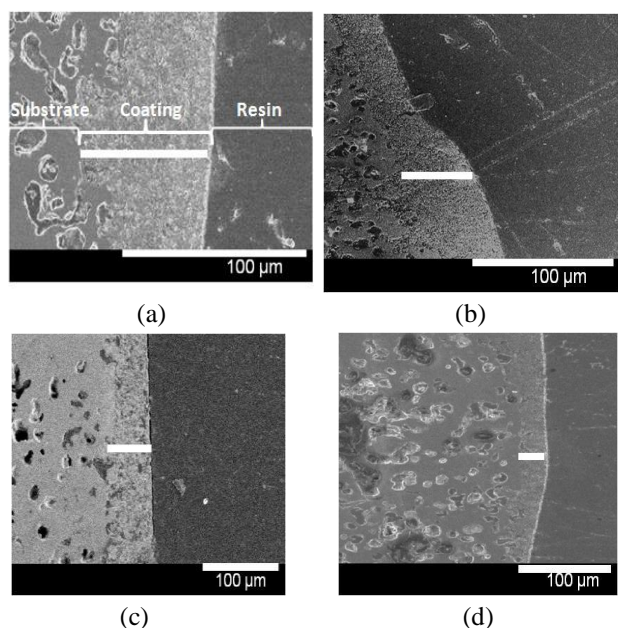


Fig.7: $\text{TiO}_2/\text{SiO}_2/\text{Al}_2\text{O}_3$ coating thickness as a function of the heat treatment temperature (a) 700°C, (b) 1000°C, (c) 1200°C, (d) 1400°C.

The figure 7 presents the SEM micrograph of $\text{TiO}_2/\text{SiO}_2/\text{Al}_2\text{O}_3$ coating cross-sections densified at different temperatures going from 700 to 1400°C, the coating thickness decreasing (from 66 μm to 25 μm) increase between 1200°C and 1400°C. At 1400 °C, the coating seems to be denser than those elaborated at lower temperature (table 1). Moreover, we also note the presence of some larger pores. These observations indicate that the coating densification occurred by grain rearrangement thanks to the silica intergranular phase viscous flow. It is in a good agreement with different studies of the glass sintering [16] and composite alumina and glass sintering [17] which show that the densification begins at temperatures higher than the glass transition temperature when the viscosity is around 10^{10} Pa.s. Due to the OH concentration of the sol-gel derived pure silica glass, a such value of viscosity has been observed at temperature lower than 1400°C [15-18]. We must note that the hardness measured for coating heating at 1400°C is still lower than the hardness of each phase and prove that a residual porosity is still present.

Table 1: Average pore diameter (μm) of coating densified at various temperatures

T(°C)	700	1000	1400
Average pore diameter (μm)	1	1,66	3,7

3.3. Na^+/Si molar ratio effect on modification of the coating $\text{TiO}_2/\text{Al}_2\text{O}_3/\text{SiO}_2$ densification temperature

To decrease the densification temperature of the $\text{TiO}_2/\text{Al}_2\text{O}_3/\text{SiO}_2$ coating that is about 1400°C as shown in section 3.2, we have changed the composition of the intergranular phase by NaCl addition in the sol-gel solution. Indeed, Na^+ ion incorporation in the network of silica gel leads to the decrease of the glass transition temperature (T_g) [19-20]. The coating microhardness evolution as a function of the temperature for five different molar ratios Na/Si (from 0.0 to 0.43) is presented in fig.8. The difference with the evolution of the hardness described in section 3.2., without NaCl addition, the micro hardness slight increasing start for a treatment temperature up to 1000 °C. Between 1000 and 1400 °C this increase is then less abrupt. NaCl modified composite coatings seem to exhibit almost the same behaviour but the main difference is that the significant increase of the hardness is noticed at lower temperature, i.e. 1200 °C, for all Na/Si ratios different from zero. From 1200°C and whatever the Na/Si ratio, the microhardness of coatings containing NaCl is always greater than the one without NaCl. This increase of the hardness at 1200°C instead of 1400°C can be explained by a better densification in 1200°C due to the presence of Na^+ ions which disrupt the SiO_2 network by decreasing the number of Si-O-Si bridge [21]. Therefore, T_g of the intergranular phase is decreased and allows the densification of the material at lower temperature.

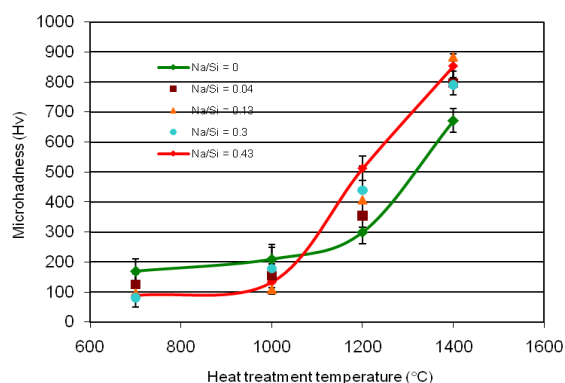


Fig.8: $\text{TiO}_2/\text{SiO}_2/\text{Al}_2\text{O}_3$ coating microhardness as a function of the heat treatment temperature for different Na/Si ratios.

Fig. 9 shows the coating microhardness as a function of the Na/Si ratio for the two highest treatment temperatures studied. The coating heated at 1200 °C exhibits an increasing microhardness when the Na/Si ratio increases while the maximum of microhardness of the coating treated at 1400 °C is reached for a Na/Si ratio of 0.13. This high microhardness value is unchanged for greater Na

amounts. This figure points out that a heat treatment at 1200 °C for 30 min is not sufficient to fully densify the coating, even for high Na/Si ratios. On the other hand, for a treatment temperature of 1400 °C, a Na/Si ratio of 0.13 allows the coating densification and thus provides to it good mechanical properties. These results are confirmed by the fig.10 that shows the microstructure of composites $\text{TiO}_2/\text{Al}_2\text{O}_3/\text{SiO}_2$ obtained without (7a) and with NaCl (at a molar ratio of 0.43 Na/Si, fig.7b). The material elaborated with NaCl addition is less porous than the one prepared without NaCl. This result shows although that the NaCl has a leak influence in the hardness of the coating. The final hardness value is higher that the hardness obtained by R.Yilmaz et al. [22] for Al_2O_3 - TiO_2 plasma sprayed.

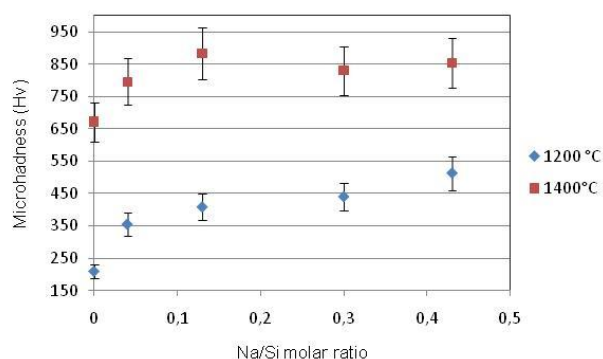


Fig.9: $\text{TiO}_2/\text{SiO}_2/\text{Al}_2\text{O}_3$ coating microhardness as a function of the Na/Si molar ratio for treatment temperatures of 1200°C and 1400°C.

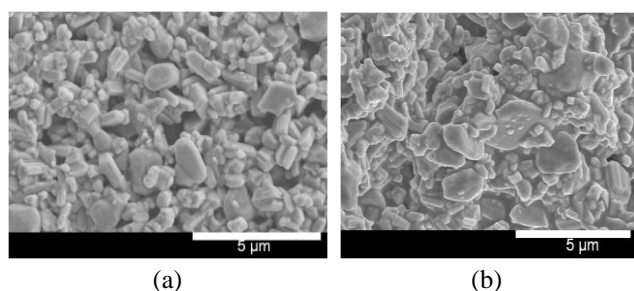


Fig.10: SEM observation of $\text{TiO}_2/\text{SiO}_2/\text{Al}_2\text{O}_3$ coatings prepared (a) with NaCl, (b) without NaCl after densification at 1200°C, $\text{Al}_2\text{O}_3/\text{TiO}_2 = 0.7$

In conclusion, NaCl addition in the sol-gel solution leads to the decrease of the intergranular phase glass transition temperature and therefore to a decrease of the densification temperature of the $\text{TiO}_2/\text{Al}_2\text{O}_3/\text{SiO}_2$ coating.

Conclusion

The objective of this study is to elaborate and to characterize a $\text{TiO}_2/\text{Al}_2\text{O}_3/\text{SiO}_2$ composite sol-gel which allows the closing pores on the ceramic substrate surface extremely porous, while improving the aesthetic aspect of

the coating by the rutile addition and by decreasing the densification temperature by NaCl addition in sol-gel solution.

The SEM observation of $\text{TiO}_2/\text{Al}_2\text{O}_3/\text{SiO}_2$ coating shows a good homogeneity without crack apparition in surface and section. Rutile and alumina are well imprisoned inside the SiO_2 matrix closing the pores surface and reduces the roughness. In order to limit the residual roughness, it is possible to making coatings of pure sol-gel of silica (without addition of powders). The elaborated coating $\text{TiO}_2/\text{Al}_2\text{O}_3/\text{SiO}_2$ presents a good adhesion to the ceramic substrate surface. After densification in 1200°C, $\text{TiO}_2/\text{Al}_2\text{O}_3/\text{SiO}_2$ coating show a low porosity after NaCl addition. The hardness measure of the composite coating densified in various temperatures shows that the heat treatment at high temperature leads to an increase of the hardness. The NaCl addition allows to decreasing the densification temperature.

References

- [1] D. Nicholson: "Using computer simulation to study the properties of molecules in micropores", J. Chem. Soc., Faraday Trans, Vol. 92(1), (1996), pp. 1–9.
- [2] S. Komarneni, V.C. Menon, R. Pidugu, J. Goworek and W. Stefaniak: "Temperature programmed desorption vs. N₂ desorption in determining pore-size distribution of mesoporous silica molecular sieves", J. Porous Mat., Vol. 3, (1996), pp. 115–119.
- [3] D.A Barrow, T.E. Petroff, R.P. Tandon, M. Sayer, Characterization of thick lead zirconate titanate films fabricated using a new sol gel based process, J. Appl. Phys., 1997, 81, 876-881.
- [4] A. Kritikaki, Fabrication of porous alumina ceramics from powder mixtures with sol-gel derived nanometer alumina: Effect of mixing method, J. Eur. Ceram. Soc., 2009, 29, 1603-1611.
- [5] T. Olding, M. Sayer, D. Barrow, Ceramic sol-gel composite coatings for electrical insulation, Thin Solid Films, 2001, 398-399, 581-586.
- [6] B.E. Yoldas, J. Mat. Sci. 12 (1977) 1203
- [7] D.A. Barrow, T.E. Petroff, M.Sayer, Thick ceramic coating using a sol gel based ceramic-ceramic 0-3 composite, Surf. Coat. Technol., 1995, 76-77, 113-118.
- [8] Ref article Mathieu et Franck.
- [9] C.J. Brinker, G.W. Scherrer, Sol-Gel Science: The Physics and Chemistry of Sol-Gel Processing, Academic, Boston, 1990.
- [10] W.C. Oliver, G.M Pharr, An improved technique for determining hardness and elastic modulus using load and displacement sensing indentation experiments, J. Mater. Res., 1992, 7, 1564-1583.

- [11] F. Petit, V. Vandeneede, F. Cambier, Relevance of instrumented micro-indentation for the assessment of hardness and Young's modulus of brittle materials, *Mater. Sci. Eng. A* 456 (2007) 252–260.
- [12] D. Siva Rama Krishna, Y. Sun, Thermally oxidised rutile-TiO₂ coating on stainless steel for tribological properties and corrosion resistance enhancement, *Appl. Surf. Sci.* 252 (2005) 1107–1116.
- [13] J.M. Antunes, A. Cavaleiro, L.F. Menezes, M.I. Simoes, J.V. Fernandes, Ultra-microhardness testing procedure with Vickers indenter, *Surf. Coat. Tech.* 149 (2002) 27-35.
- [14] A. Chmel, T. Pesina, V.S. Shashkin, Structural correlation and structural relaxation at the final stage of gel-to-glass transition in silica, *J. Non- crystalline. Sol.*, 210 (1997) 254-260.
- [15] C. Zoller, caractérisation de préformes sol-gel en vue de réaliser des fibres dopées par des nanoparticules semi-conductrices, mémoire de thèse, 2007.
- [16] A. Karamanov, M. Aloisi, M. Pelino, Sintering behaviour of a glass obtained from MSWI ash, *J. Eur. Ceram. Soc.*, 25 (2005) 1531-1540.
- [17] M. Eberstein, S. Reinsch, R. Muller, J. Deubener, W. A. Schiller, Sintering of glass matrix composites with small rigid inclusions, *J. Eur. Ceram. Soc.*, 29(2009) 2469-2479.
- [18] K. Yamahara, K. Shima, A. Utsunomiya, Y. Tsurita, Viscosity of silica glass prepared from sol-gel powder, *J. Non- crystalline. Sol.*, 349 (2004) 341-346.
- [19] S. Muthupari, K.J. Rao, Cluster model of glass transition. The variation of T_g with cage vibrational frequency of Na⁺ ions sodium borovanadate glasses, *Chem. Phys. Lett.*, 1994, 223, 133-138.
- [20] H. Roggendorf, D. Boschel, Glass transition in dried aqueous sols, *J. Non- crystalline. Sol.*, 351(2005) 957-961.
- [21] J. Zarazycki, *les verres et l'état vitreux*, Masson, 1982.
- [22] R. Yilmaz, A.O. Kurt, A. Demir, Z. Tatli, Effects of TiO₂ on the mechanical properties of the Al₂O₃–TiO₂ plasmasprayed coating.